Morphologies of Blends of Isotactic Polypropylene and Ethylene Copolymer by Rapid Expansion of Supercritical Solution and Isobaric Crystallization from Supercritical Solution

S. J. HAN,[1,2] D. J. LOHSE,[1] M. RADOSZ,[3] L. H. SPERLING[2,4–7]

[1] Exxon Research and Engineering Company, Route 22 East, Annandale, New Jersey 08801

[2] Center for Polymer Science and Engineering, Lehigh University, Bethlehem, Pennsylvania 18015-3194

[3] Department of Chemical Engineering and Macromolecular Studies Group, Louisiana State University, Baton Rouge, Louisiana 70803-7303

[4] Department of Chemical Engineering, Lehigh University, Bethlehem, Pennsylvania 18015-3194

[5] Department of Materials Science and Engineering, Lehigh University, Bethlehem, Pennsylvania 18015-3194

[6] Polymer Interfaces Center, Lehigh University, Bethlehem, Pennsylvania 18015-3194

[7] Materials Research Center, Lehigh University, Bethlehem, Pennsylvania 18015-3194

Received 9 November 1999; accepted 3 December 1999

ABSTRACT: Isotactic polypropylene (iPP) and ethylene-butene (EB) copolymers were dissolved in supercritical propane and precipitated by rapid expansion of supercritical solution (RESS) and isobaric crystallization from SS (ICSS). The cloud-point pressures of the ternary solutions were found to increase as the immiscibility of PP and EB copolymer increased (i.e., as the number of ethyl branches in the EB copolymers decreased). The RESS process resulted in microfibers and a trace of microparticles, and the EB copolymer domains in the blends decreased in size as the ethyl branch content in the EB copolymers increased. The thermal stability of the copolymer domains was improved by synthesizing thermoplastic vulcanizate (TPV) from PP and ethylene-propylene-diene terpolymer in a supercritical propane solution followed by RESS. The ICSS process produced microcellular polymeric foamlike materials, but the two polymers were precipitated independently by thermally induced phase separation. © 2000 John Wiley & Sons, Inc. J Appl Polym Sci 77: 1478–1487, 2000

Key words: polymer blends; supercritical propane; rapid expansion of supercritical solution; isobaric crystallization from SS; morphology

INTRODUCTION

Supercritical fluid processes have recently been applied to polymers, resulting in unique morphologies. The new processing methods involve rapid expansion of supercritical solution (RESS),[1–6] supercritical antisolvent (SAS),[7,8] isobaric crystallization from SS (ICSS),[9,10] microcellular foam by the critical point drying process,[11,12] blends prepared by supercritical carbon dioxide swelling,[13] thermoplastic vulcanizate (TPV) synthesis in SS,[14] as well as other microcellular foam processes with supercritical fluids.[15,16]

Correspondence to: S. J. Han (hansj@ucarb.com).

Journal of Applied Polymer Science, Vol. 77, 1478–1487 (2000)

Table I Characteristics of Polymers

Sample	M_w	Polydispersity	T_m (°C)	Density at 23°C (g/mL)
EB9	94,900	2.0	98	0.8986
EB23	87,200	1.1	46	0.8573
EB60	86,000	1.1	Amorphous	0.8648
EPDM	198,000	2.0	45	0.8940
PP	91,000	2.0	161	0.9065

The common features of these processes involve dissolving or saturating a polymer in a suitable subcritical or supercritical fluid and then precipitating it by triggering nucleation of the polymer via a variety of phase separation mechanisms, which are controlled by adjusting process conditions such as pressure and temperature, or reaction in supercritical fluids. The types of morphology obtained from these processes are microporous fibers, microparticles, and cellular foam-like materials.

There has been growing interest in improving the impact strength of polypropylene (PP). Typically, PP has been blended with rubbery polymers (e.g., ethylene-propylene copolymers) by melt mixing.[17,18] The impact strength is known to increase as rubber particle size is reduced.[19] The rubber particle size can be controlled by careful matching of the viscosity of two polymers.[20] However, PP has a lower melt viscosity than ethylene copolymers of the same molecular weight so that selecting PP and ethylene copolymer pairs with matching viscosity is limited and it is sometimes inconvenient to do so. Thomann et al. studied the melt miscibility of isotactic PP (iPP) with ethylene-butene (EB) copolymers as a function of 1-butene content to enhance the toughness of the blends by controlling the adequate compatibility between two polymers and reported that iPP was melt miscible with EB copolymers for a 1-butene content of approximately 88 wt %.[21]

The objectives of this study are to blend EB copolymers and PP in supercritical propane solution and to investigate the morphology of the polymer blends by processing the solutions via RESS and ICSS. The approach involves measuring the phase behavior of ternary solutions with a variable volume optical batch cell and then processing the solution directly from the batch cell through a connecting spray unit for the RESS, which involves the pressure quenching method. By comparison, a thermal quenching method (cooling the solution isobarically from the homogenous solution) involves crossing the solid–liquid transition for the ICSS. The melting transitions for the polymers resulting from each process are analyzed with differential scanning calorimetry (DSC). The morphological characteristics are investigated with scanning electron microscopy (SEM). The main advantages of using supercritical fluids to process the polymers are the easy removal of the solvent from the polymer product, the easy recycling of the solvent, and fine control of the polymer morphology by various phase disengagement routes.

EXPERIMENTAL

Materials

The iPP was synthesized with a metallocene catalyst. The EB copolymers were classified in terms of their mole percent of butene comonomer, which was characterized by ^{1}H-NMR. The EB9 was synthesized with a metallocene catalyst. EB23 and EB60 were hydrogenated polybutadienes synthesized with an anionic initiator in the presence of a polar modifier to control the vinyl content.[22] The number following the EB indicates the mole fraction of 1-butene in the EB copolymer. EB9 is a semicrystalline polymer and EB23 has a trace of crystallinity, while EB60 is an amorphous polymer. Ethylene-propylene-diene (EPDM) is a statistical terpolymer, which has 70 wt % ethylene, 23–27 wt % propylene, and 3–7 wt % ethylidene norbornene. The characteristics of the polymer samples used in this work are summarized in Table I. Solvent propane (99.9%) was obtained from Matheson Gas Co., and *tert*-butyl peroxide (99.4% purity) was obtained from Aldrich Chemical Co. Both were used without purification.

Apparatus and Procedure

Phase transitions of the polymer solutions were determined with a high pressure variable volume

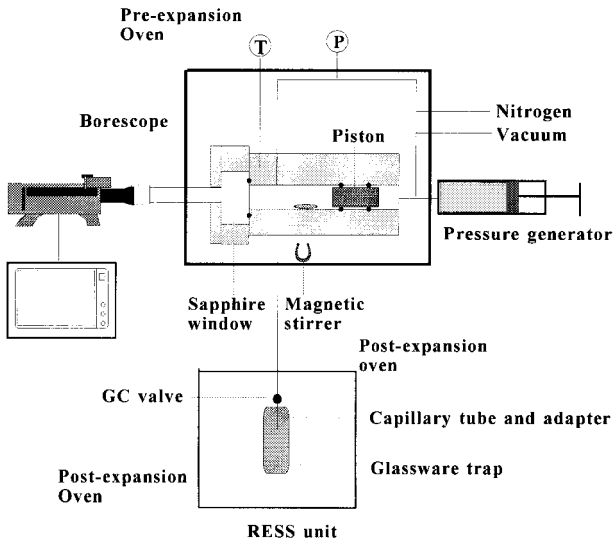

Figure 1 A schematic of a high pressure optical batch cell and the RESS unit.

optical batch cell unit described in detail elsewhere.[23,24] For the cloud-point determination (liquid–liquid transition), known amounts of two polymers were inserted into the cell and then charged with propane solvent at room temperature. The solution was heated above the melting temperatures of the polymers in the preexpansion oven and pressurized by a piston to a homogeneous solution while stirring. After equilibrium, the pressure was slowly lowered under isothermal conditions by withdrawing the piston. The cloud-point pressure was the pressure where the solution became completely hazy. For the solid–liquid transition, the solution was heated and pressurized to a homogenous solution well above the melting temperatures of the polymers. Then the solution was isobarically cooled below the crystallization temperature of the polymers until the solution became hazy. The solid–liquid transition temperatures recorded were below the crystallization temperature of the polymers that was determined by DSC.

The high pressure optical batch cell unit was modified by the spraying unit for the RESS process as shown in Figure 1. The spraying unit consisted of 1.58-mm o.d. stainless tubing with a 0.254-mm i.d. (Valco Instruments Co. Inc.), a zero dead volume chromatographic valve (Valco Instruments Co. Inc.), and a fused silica capillary tube (Chrompack). The 1.58-mm o.d. tube line was insulated and maintained at the same constant temperature as the preexpansion oven temperature by using heating tape and a thermocouple. The fused silica capillary tube was directly connected to the valve with the fused silica adapter that consisted of two components: a liner that slides over the fused silica tubing and a ferrule. Both of them were made of polyimide (Valco Instruments Co. Inc.). The i.d. of the silica tube was 75 μm, and the length of the silica tube was approximately 2.5 cm. For the RESS experiment of the TPV gel, 125-μm i.d. stainless tubing (Valco Instruments Co. Inc.) was used.

In the RESS process a homogenous solution in the cell inside the preexpansion oven was pressure quenched on a time scale of microseconds,[4] spraying the solution into the ambient pressure in the postexpansion oven through a fused silica tube. During the RESS process the polymer solution in the cell was maintained as a homogeneous solution to keep the polymer concentration constant by limiting each sampling time to less than a few seconds. The precipitated polymers were collected by a glassware trap in the postexpansion oven. For the RESS process of the TPV gel a homogenous polymer solution was crosslinked at 175°C and 650 bar for 1 h by injecting *tert*-butyl peroxide through a feed line, followed by rapid expansion of the solution at the same temperature to ambient pressure. The detailed setup and TPV synthesis conditions were reported elsewhere.[14] In the ICSS process a homogeneous solution above the melting point of the two polymers was cooled and crystallized at a temperature below the solid–liquid transition of PP under isobaric conditions. After the polymer precipitated because of crystallization, the solvent in the cell was slowly released to ambient pressure and then dried. The precipitated polymer blends were collected from the cell for further examination. The processing paths for the RESS, ICSS, and TPV synthesis are shown in Figure 2.

Microscopy Analysis

The morphological characteristics of precipitated polymers were studied by scanning microscopy (Jeol JSM-35C and JSM-6320F). Prior to the SEM study, the samples were coated with gold–palladium to a thickness of 10 nm by a sputter coater (Hummer X, Anatech Ltd.). The PP sample was analyzed without coating with a field emission SE microscope at 1 kV. Phase contrast optical microscopy with polarizers (Leitz, Inc.) was also applied to investigate the morphology of polymer blends made into thin films.

DSC Analysis

The melting transition behavior of the polymers was studied with a DS calorimeter (Seiko,

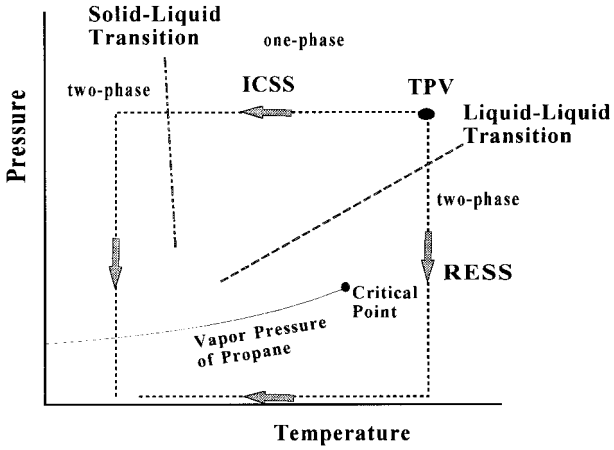

Figure 2 The processing paths of RESS, ICSS, and TPV synthesis.

RDC220). The sample was heated from −110 to 200°C at a heating rate of 10°C/min. The melting temperature was taken as the melting peak endotherm in the DSC thermogram.

RESULTS AND DISCUSSION

Phase Behavior of Binary and Ternary Systems

The cloud-point pressures of the phase diagram determine the minimum pressure required to maintain a homogeneous polymer solution. Figures 3–5 illustrate the phase behavior of binary and ternary polymer solutions in propane based on this cloud-point pressure data. As the number of ethyl branches in the EB copolymers increases, the cloud-point pressures of EB copolymers in the binary solutions of propane decrease and the type of phase transition changes from upper critical solution temperature (UCST) type behavior [i.e., $(\partial P/\partial T)_x < 0$] to lower critical solution temperature type behavior [i.e., $(\partial P/\partial T)_x > 0$]. The short chain branching effects on the cloud-point pressures of ethylene copolymers in the binary solutions of propane were investigated in detail by

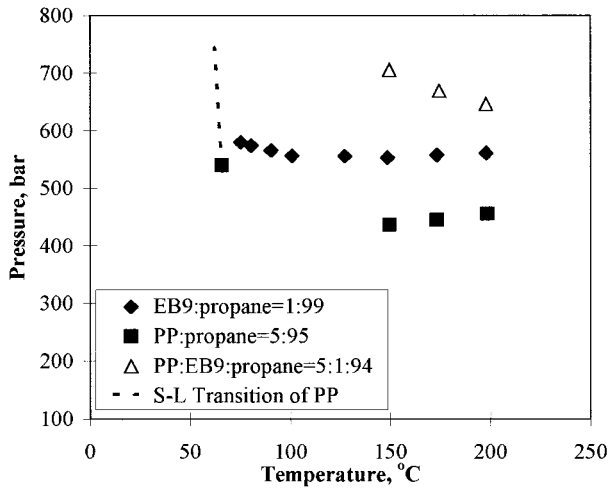

Figure 3 A binary and ternary pressure–temperature diagram for EB9 and propane, PP and propane, and EB9, PP, and propane at various compositions (wt %); S-L, solid–liquid transitions of PP.

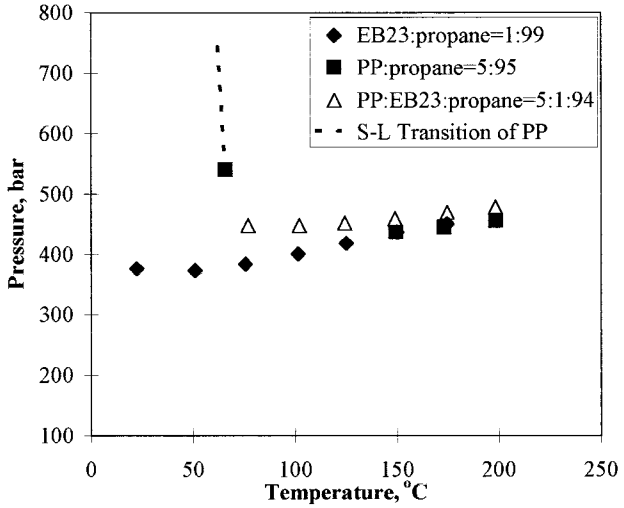

Figure 4 A binary and ternary pressure–temperature diagram for EB23 and propane, PP and propane, and EB23, PP, and propane at various compositions (wt %); S-L, solid–liquid transitions of PP.

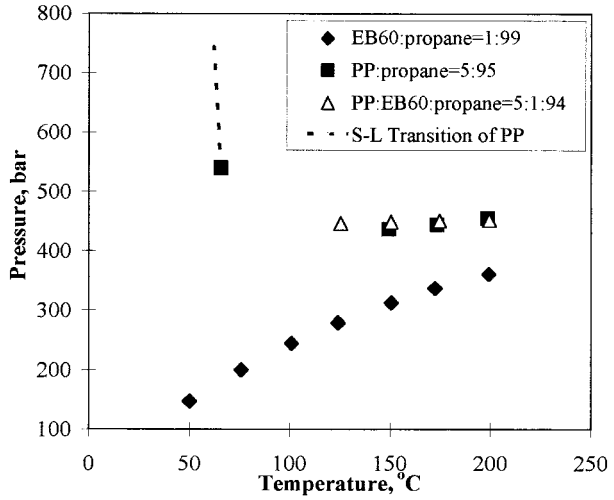

Figure 5 A binary and ternary pressure–temperature diagram for EB60 and propane, PP and propane, and EB60, PP, and propane at various compositions (wt %); S-L, solid–liquid transitions of PP.

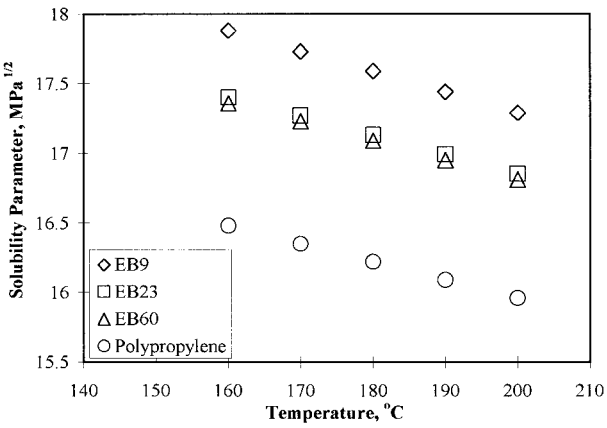

Figure 6 Solubility parameters of the polymers between 160 and 200°C.

Han et al.[24] In short, as the solubility parameters of ethylene copolymers decreased, their cloud-point pressures decreased. The solubility parameters of EB copolymers and PP are shown in Figure 6. The solubility parameters were calculated from the internal pressure of the polymers using experimental thermal expansion coefficients and compressibility.[25] As the number of short chain branches increased in the polymers, the solubility parameters decreased in the temperature range of 160–200°C. The solubility parameters of a wide range of polyolefins are summarized elsewhere.[26]

The cloud-point pressures of the ternary solutions investigated were higher than the binary solutions at the compositions used in the ternary systems. This was because the two polymers were thermodynamically immiscible, causing the mutual solubility of the ternary solution to be decreased. The short chain branching effect also influenced the phase behavior of the ternary systems. The cloud-point pressures of the ternary solutions also decreased from about 650 to about 450 bar as the number of ethyl branches increased in the EB copolymer in the ternary systems, then became substantially constant for EB23 and EB60 as also seen in comparing Figures 3–5.

The solid–liquid transition of PP in the binary solution was determined by isobaric cooling. Initially, the solution was a homogeneous solution at 170°C and 550 bar or higher. On cooling, the solid–liquid transition occurred near 65°C, essentially independent of pressure. Because the normal melting temperature of the iPP is 161°C, the melting temperature of the PP was lowered because of the plasticization effect of excess propane. The solid–liquid transitions of ternary systems including EB23 and EB60 also showed values very close to that of the binary system of PP in propane, suggesting that PP precipitated independently from the solutions while EB23 and EB60 remained in solution. It must be noted that the ternary solution including EB9 showed a UCST type phase behavior at 150°C or above so that liquid–liquid phase separation occurred on cooling before the solid–liquid transition of PP.

Morphology of Polymer Blends by RESS

Solutions of PP and EB copolymer in propane were heated above 150°C and pressurized until they became homogeneous. The RESS unit and the postexpansion oven temperature were maintained at the same temperature as the preexpansion oven. As Mawson et al.[6] reported for a RESS system of crystalline fluoropolymers in carbon dioxide, microfibers dominant the morphology of resulting polymer blends when a high ratio of length over nozzle diameter ($L/D > 300$) was used. The RESS experimental conditions are summarized in Table II for a capillary i.d. of 75 μm and L/D of 330 for the nozzle.

During the RESS process, the solutions in the cell were maintained as one phase to keep the polymer concentration constant by limiting the RESS sampling time to less than a few seconds. The actual phase separations occur in the capillary nozzle in microseconds, followed by the ex-

Table II RESS Experimental Conditions and Morphology of Polymer Blends

Ternary Solution Composition	$T_{\text{preexpansion}}$ (°C)	$P_{\text{preexpansion}}$ (bar)	Morphology
PP : EB9 : propane = 5 : 1 : 94	175	700	Fibrils
PP : EB23 : propane = 5 : 1 : 94	151	600	Fibrils
PP : EB60 : propane = 5 : 1 : 94	175	600	Fibrils
PP : EPDM : propane = 4 : 1 : 94 (TPV)	175	680	Fibrils

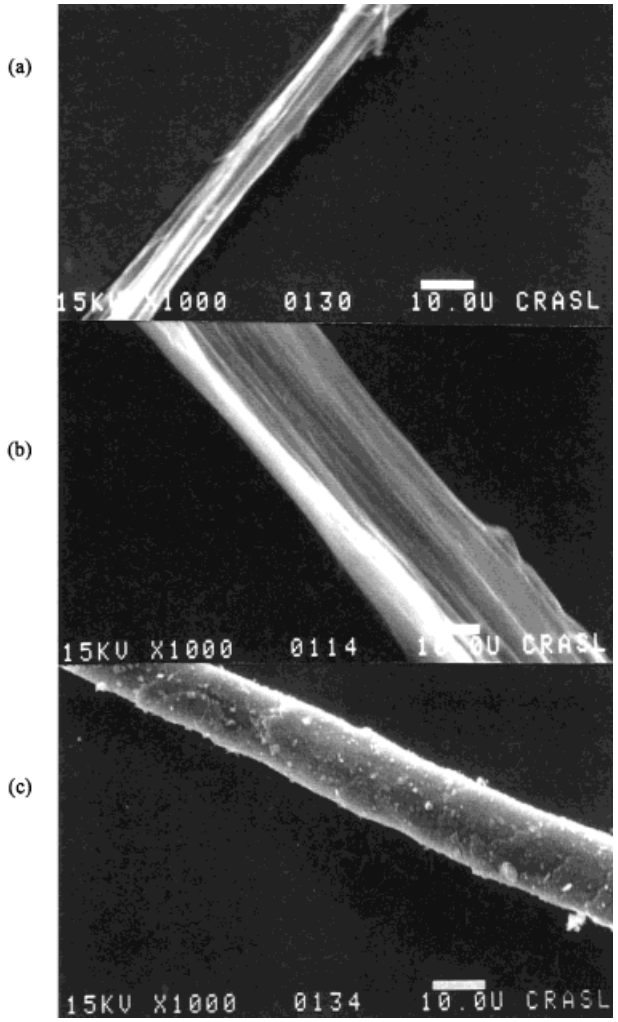

Figure 7 Surface morphologies of blended fibers by the RESS process: (a) PP : EB9 = 5 : 1, (b) PP : EB23 = 5 : 1, and (c) PP : EB60 = 5 : 1.

pansion of propane because of the large pressure drop at the tip of the nozzle. The high L/D ratio, the processing temperatures, and high gas flow imposed high shearing stresses on the polymer melt, which was subsequently drawn into short fibers. Typical examples of blended fibers produced by the RESS process are presented in Figure 7. The diameter of the fibers ranged from approximately 10–50 μm. The surface of the fibers showed oriented microfibrils in the direction of shear flow, which again suggested the orientation of polymer chains in the capillary nozzle by the shearing action.

The microfibers were melted between two glass slides at 190°C for 2.5 min to form a film and cooled to ambient temperature to study the bulk phase morphology. Figure 8 illustrates the phase morphology of the RESS-process polymer blends

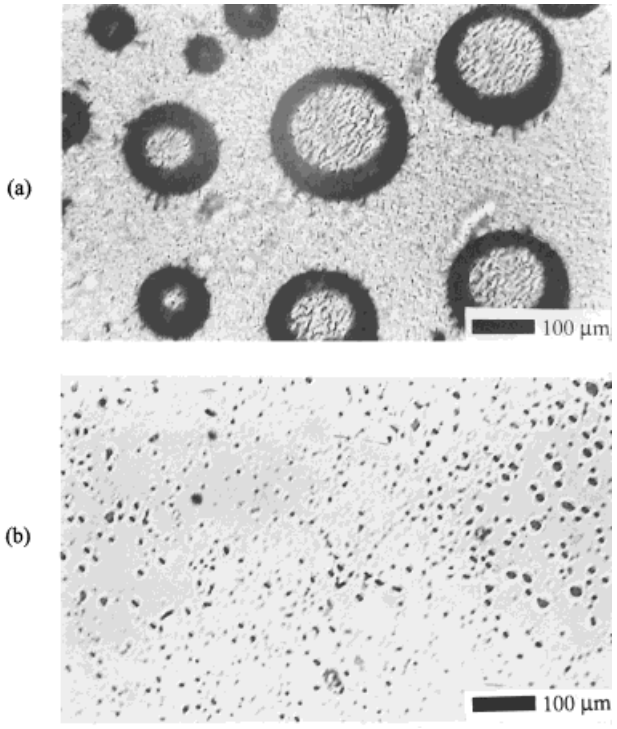

Figure 8 Phase morphologies of polymer blends by the RESS process after annealing in a 190°C oven for 2.5 min: (a) PP : EB9 = 5 : 1 and (b) PP : EB60 = 5 : 1.

via phase contrast optical microscopy. The polymer blends were phase separated and the domain sizes of the minor EB copolymer decreased in the blends as the concentration of ethyl branches increased, suggesting better miscibility of the two polymers. The DSC thermograms in Figures 9–11

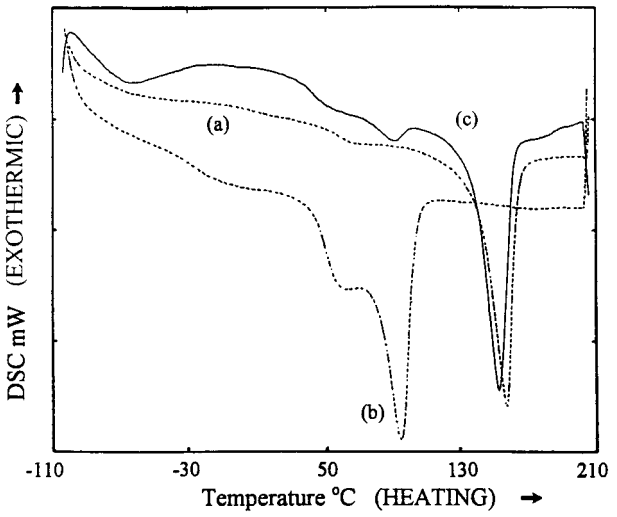

Figure 9 DSC thermograms of polymer blends by the RESS process: (a) PP, (b) EB9, and (c) PP : EB9 = 5 : 1.

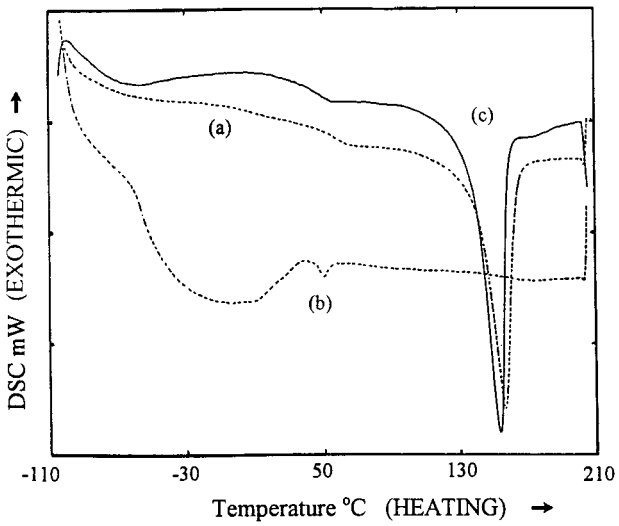

Figure 10 DSC thermograms of polymer blends by the RESS process: (a) PP, (b) EB23, and (c) PP : EB23 = 5 : 1.

showed slight depressions of PP melting peaks in the blends after film formation, suggesting limited mixing. The thermal transitions of minor components in the blends were also evident in the DSC thermograms, suggesting that phase separation by thermodynamic immiscibility was still dominating the process. The portion of miscible EB copolymers in iPP is calculated from the melting point depression relationship[27] expressed by

$$1/T_f - 1/T_f^0 = (R/\Delta H_f)X_B \quad (1)$$

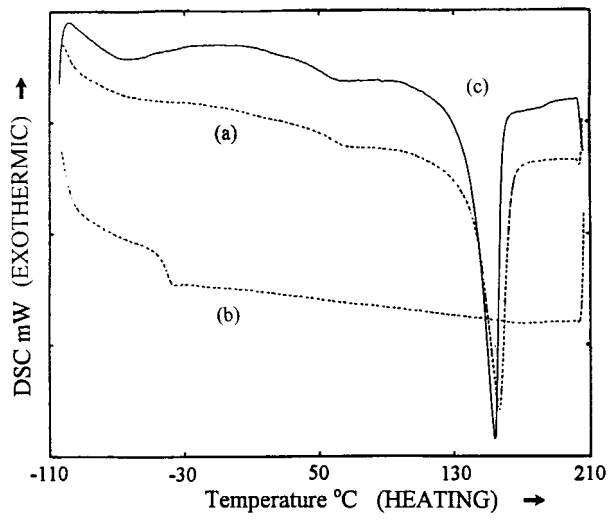

Figure 11 DSC thermograms of polymer blends by the RESS process: (a) PP, (b) EB60, and (c) PP : EB60 = 5 : 1.

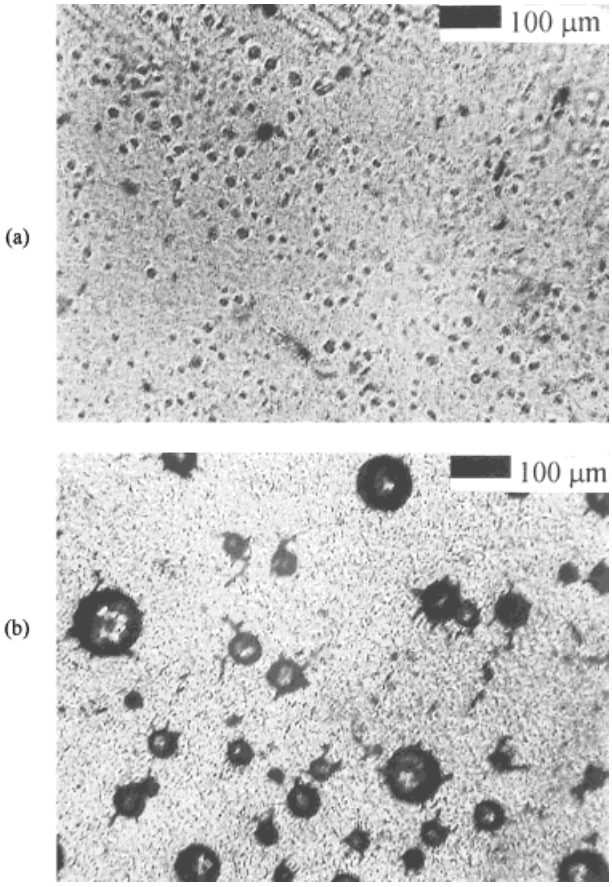

Figure 12 Phase morphologies of polymer blends (PP : EB23 = 5 : 1) by the RESS process after annealing in a 190°C oven for (a) 2.5 or (b) 5 min.

$$X_B = (1/T_f - 1/T_f^0)(\Delta H_f/R) \quad (2)$$

where T_f, T_f^0, R, ΔH_f, and X_B are the melting point of the polymer, the melting point of the pure crystalline polymer, the gas constant, the heat of melting transition, and a mole fraction of the impurity (i.e., the part of the EB copolymer miscible with PP). The melting-point depression calculations suggest that at most 0.1–0.2 mol % of the EB copolymers was dissolved in the crystalline portion of the iPP after the RESS experiments.

Thermal stability of RESS-process blends was examined by annealing a blend sample at 190°C. Figure 12 shows the coarsening of EB23 domains after aging at 190°C for 2.5 versus 5 min. Although EB copolymer domain sizes can be reduced by blending PP with EB copolymer with a high ethyl branch content, thermodynamic immiscibility between the two polymers leads to phase separation, eventually resulting in larger domains in the blends. To improve the thermal

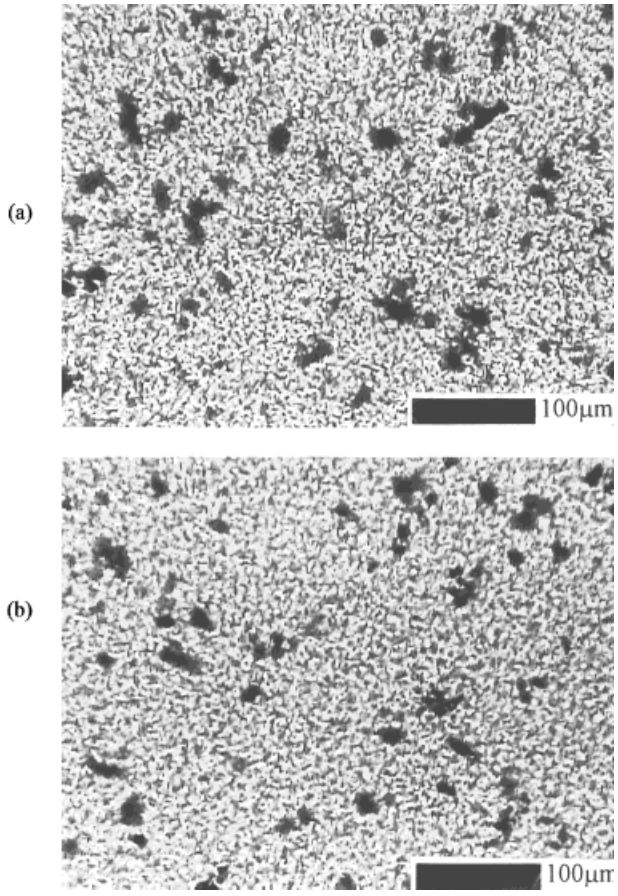

Figure 13 Phase morphologies of TPV (PP : EPDM = 4 : 1) by the RESS process after annealing in a 190°C oven for (a) 5 or (b) 30 min.

stability of the EB copolymer domains, TPV from PP and EPDM was synthesized in supercritical propane, followed by RESS. The TPV gel solution also produced microfibers very similar to other blends by the RESS process. The RESS-processed TPV did not show any significant coarsening of rubbery EPDM domains after aging at 190°C for 30 min because of the crosslinking of rubbery domains as in Figure 13.

Morphology of Polymer Blends by ICSS

The ICSS conditions are summarized in Table III. The ICSS process produced the microcellular foamy morphology as shown in Figure 14. The microcellular foam consists of porous microspheres in the range of 10–50 μm. This microcellular foamy structure can be explained by the following mechanism. Initially, the PP in the homogeneous SS starts to form nuclei as the system is thermally induced to crystallize by cooling below the solid–liquid transition. Then the EB polymers precipitate as the isobaric cooling continues. The solvent propane plasticized the microspheres and they were welded together by coalescence. The evaporation of the propane at the final step resulted in microcellular foams as shown in the Figure 14. EB9 appeared as a coating of microparticles on top of the PP foam. EB23 partially covered the PP foam, and EB60 nearly completely covered the surface of the PP foam. These electron micrographs suggest that the PP precipitated first during the ICSS process and was followed by the precipitation of EB copolymers on the final reduction of the pressure. The EB9 resulted in powdery flakes because of its crystallinity, while other EB copolymers were viscous because they were nearly amorphous or amorphous. The morphology of pure iPP is shown in Figure 15. The pore radii of PP microspheres range from approximately 50–100 nm. Whaley et al.[28] recently showed that the microspheres consist of a dense core and dendritic porous structures. In important ways, the microspheres resemble prototype spherulites. It is likely that the lamellae grow outward, resulting in the porous structure.

CONCLUSIONS

The mixing of short chain branched EB copolymers and iPP in supercritical propane solutions

Table III ICSS Experimental Conditions and Morphology of Polymer Blends

Ternary Solution Composition	$T_{initial}$ (°C)	$P_{initial}$ (bar)	T_{ICSS} (°C)	P_{ICSS} (bar)	Morphology
PP : EB9 : propane = 5 : 1 : 94	175	700	55	700	Powdery coating on cellular foam
PP : EB23 : propane = 5 : 1 : 94	175	600	60	600	Partial layer coating on cellular foam
PP : EB60 : propane = 5 : 1 : 94	175	600	55	600	Complete layer coating on cellular foam

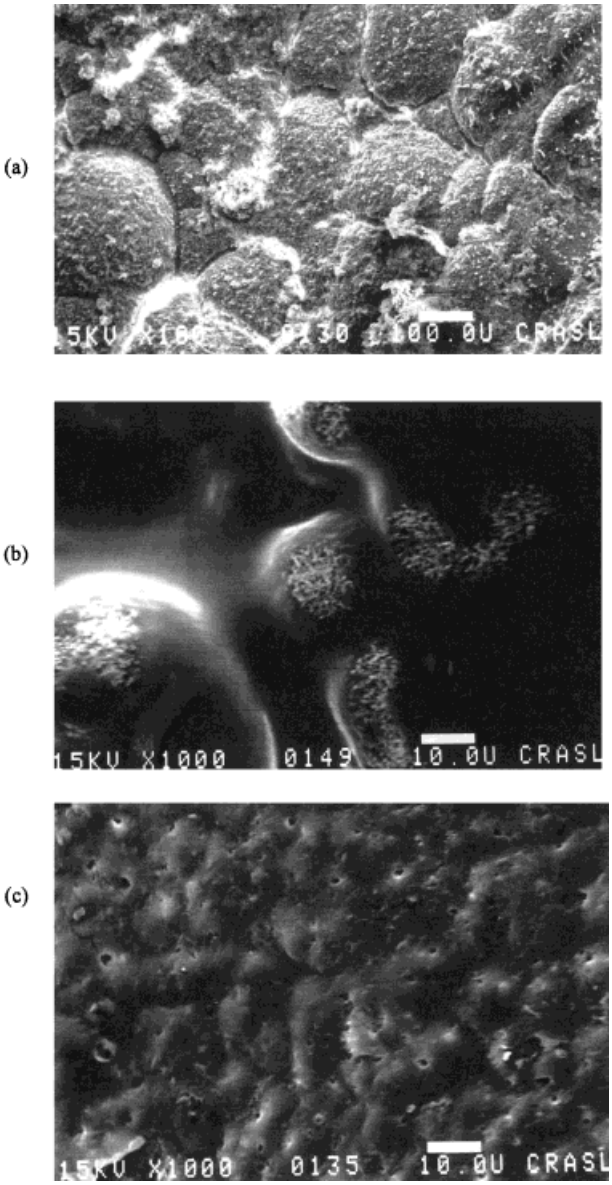

Figure 14 Surface morphologies of polymer blends by the ICSS process: (a) PP : EB9 = 5 : 1, (b) PP : EB23 = 5 : 1, and (c) PP : EB60 = 5 : 1.

produced strong effects on the cloud-point pressures of these materials in binary and ternary solutions. The cloud-point pressures of ternary solutions were higher than the corresponding binary solutions of the same concentration and increased as the ethyl branch fraction in the EB copolymers decreased.

The RESS process resulted in 10–60 μm diameter microfibers. The phase domain sizes of EB copolymers in the blends from the RESS process decreased as the content of ethyl branches in the EB copolymers increased. According to the DSC study, the melting temperatures of EB copolymers and PP were changed only modestly, indicating only a slight thermodynamic miscibility of the two polymers. The RESS-processed TPV showed reduced domain growth of rubbery domains due to the crosslinking of EPDM. The ICSS process resulted in microcellular polymeric foams, which were phase separated. Each polymer was precipitated independently by the thermally induced phase separation.

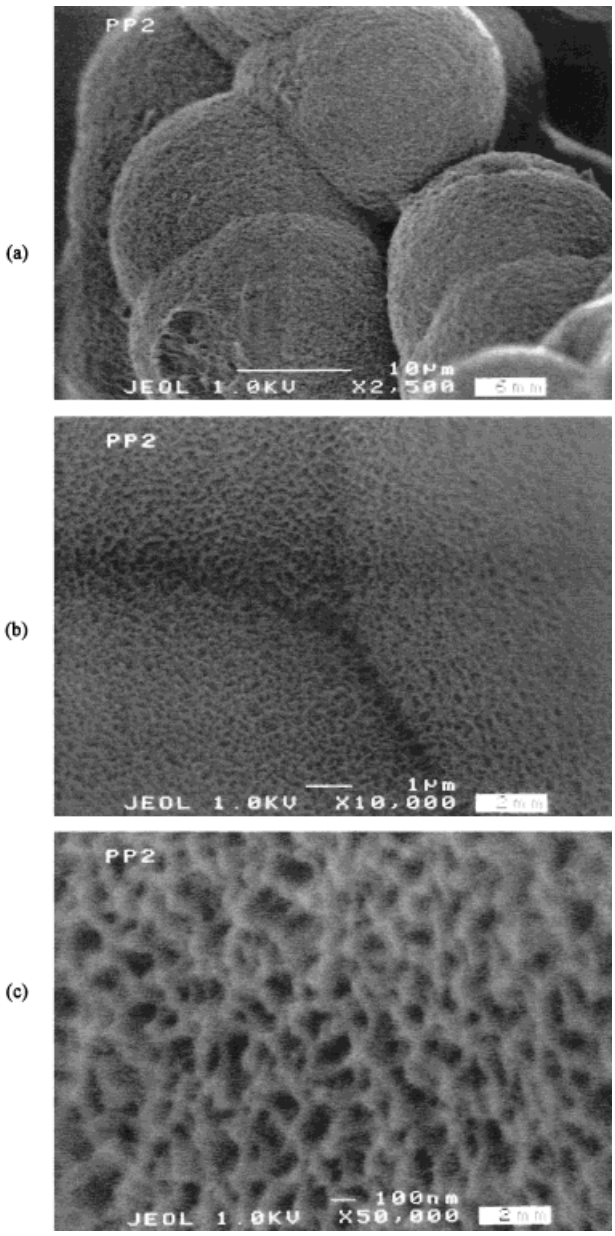

Figure 15 Surface morphologies of iPP by the ICSS process (10 wt % solution at 25°C and 500 bar): (a) microspheres, (b) the interface between microspheres, and (c) the porous surface of the microsphere.

REFERENCES

1. Matson, D. W.; Peterson, R. C.; Smith, R. D. Mater Lett 1986, 4, 429.
2. Smith, R. D. U.S. Pat. 4,582,731, 1986.
3. Tom, J. W.; Debenedetti, P. Biotechnol Prog 1991, 7, 403.
4. Tom, J. W.; Debenedetti, P. J Aerosol Sci 1991, 22, 555.
5. Lele, A. K.; Shine, A. D. Ind Eng Chem Res 1994, 33, 1476.
6. Mawson, S.; Johnston, K. P.; Combes, J. R.; DeSimone, J. M. Macromolecules 1995, 28, 3182.
7. Yeo, S.-D.; Debenedetti, P. G.; Radosz, M.; Schmidt, H.-W. Macromolecules 1993, 26, 6207.
8. Dixon, D. J.; Johnston, K. P. J Appl Polym Sci 1993, 50, 1929.
9. Bush, P. J.; Pradhan, D.; Ehrlich, P. Macromolecules 1991, 24, 1439.
10. Pradhan, D.; Ehrlich, P. J Polym Sci Part B Polym Phys 1995, 33, 1053.
11. Srinivasan, G.; Elliott, J. R. Ind Eng Chem Res 1992, 31, 1414.
12. Pekara, R. W.; Stone, R. E. Polym Prepr 1988, 29, 204.
13. Kung, E.; Lesser, A. J.; McCarthy, T. J. Macromolecules 1998, 31, 4160.
14. Han, S. J.; Lohse, D. J.; Radosz, M.; Sperling, L. H. Macromolecules 1998, 31, 16, 5407.
15. Goel, S. K.; Beckman, E. J. Polym Eng Sci 1994, 34, 1137.
16. Baldwin, D. F.; Park, C. B.; Suh, N. P. Polym Eng Sci 1996, 36, 1437.
17. Yamaguchi, M.; Miyata, H.; Nitta, K. J Appl Polym Sci 1996, 62, 87.
18. Ramsteiner, F.; Kanig, G.; Heckmann, W.; Gruber, W. Polymer 1983, 24, 365.
19. Speri, W. M.; Patrick, G. R. Polym Eng Sci 1975, 15, 668.
20. Van Der Wal, A. Ph.D. Dissertation, University of Twente, The Netherlands, 1996.
21. Thomann, Y.; Suhm, J.; Thomann, R.; Bar, G.; Maier, R.-D.; Mulhaupt, R. Macromolecules 1998, 31, 5441.
22. Morton, M.; Fetters, L. J. Rubber Chem Technol 1975, 48, 359.
23. Chen, S.-J.; Randelman, R. E.; Seldomridge, R. L.; Radosz, M. J Chem Eng Data 1993, 38, 211.
24. Han, S. J.; Lohse, D. J.; Radosz, M.; Sperling, L. H. Macromolecules 1998, 31, 8, 2533.
25. Graessley, W. W.; Krishnamoorti, R.; Balsara, N. P.; Butera, R. J.; Fetters, L. J.; Lohse, D. J.; Schultz, D. N.; Sissano, J. A. Macromolecules 1994, 27, 3896.
26. Han, S. J.; Lohse, D. J.; Condo, P. D.; Sperling, L. H. J Polym Sci Polym Phys 1999, 37, 2835.
27. Sperling, L. H. Introduction to Physical Polymer Science, 2nd ed.; Wiley: New York, 1992; p 253.
28. Whaley, P. D.; Kulkarni, S.; Ehrlich, P.; Stein, R. S.; Winter, H. H.; Conner, W. C.; Beaucage, G. J Polym Sci Polym Phys 1998, 36, 617.